

# Heterologous expression of *PtAAS1* reveals the metabolic potential of the common plant metabolite phenylacetaldehyde for auxin synthesis *in planta*

Jan Günther<sup>1,3,\*</sup>, Rayko Halitschke<sup>2</sup>, Jonathan Gershenzon<sup>1</sup> and Meike Burow<sup>3</sup>

<sup>1</sup>Max Planck Institute for Chemical Ecology, Department for Biochemistry, Hans-Knöll-Strasse 8, D-07745 Jena, Germany

<sup>2</sup>Max Planck Institute for Chemical Ecology, Department for Molecular Ecology, Hans-Knöll-Strasse 8, D-07745 Jena, Germany

<sup>3</sup>Department of Plant and Environmental Sciences, University of Copenhagen, Thorvaldsensvej 40, 1871 Frederiksberg C, Denmark

## Contact

Affiliation 1; [jg@plen.ku.dk](mailto:jg@plen.ku.dk), [gershenzon@ice.mpg.de](mailto:gershenzon@ice.mpg.de)

Affiliation 2; [rhalitschke@ice.mpg.de](mailto:rhalitschke@ice.mpg.de)

Affiliation 3; [jg@plen.ku.dk](mailto:jg@plen.ku.dk), [mbu@plen.ku.dk](mailto:mbu@plen.ku.dk)\*

Author to contact for correspondence: [jg@plen.ku.dk](mailto:jg@plen.ku.dk); Twitter: @JanGnther18

ORCID IDs: 0000-0001-8042-5241 (J.Gü.); 0000-0002-1109-8782 (R.H.); 0000-0002-1812-1551 (J.Ge.); 0000-0002-2350-985X (M.B.)

**Author Contributions:** J.Gü. and J.Ge. designed research. J.Gü., carried out the experimental work, analyzed data and wrote the manuscript. R.H. analyzed samples via untargeted Lc-qToF-MS/MS. J.Ge. and M.B. contributed to and finalized the manuscript. All authors read and approved the final manuscript.

**Funding:** The research was funded by the Max-Planck Society and Novo Nordisk Fonden (NNF200C0065026).

**Acknowledgments:** We thank Tamara Krügel, Danny Kessler, and all the MPI-CE gardeners for their help with rearing the poplar and *Nicotiana benthamiana* plants. D. Werck-Reichhart, Strasbourg, France, is thanked for kindly providing the pCAMBIA vectors and for the nice introduction to the USER cloning system.

**Conflicts of Interest:** The authors declare no conflict of interest.

## Running Title: Defense metabolite biosynthesis leads to auxin formation

**Abstract:** Aromatic aldehydes and amines are common plant metabolites involved in several specialized metabolite biosynthesis pathways. Recently, we showed that the aromatic aldehyde synthase *PtAAS1* and the aromatic amino acid decarboxylase *PtAADC1* contribute to the herbivory-induced formation of volatile 2-phenylethanol and its glucoside 2-phenylethyl- $\beta$ -D-glucopyranoside in *Populus trichocarpa*. To gain insights into alternative metabolic fates of phenylacetaldehyde and 2-phenylethylamine beyond alcohol and alcohol glucoside formation, we expressed *PtAAS1* and *PtAADC1* heterologously in *Nicotiana benthamiana* and analyzed plant extracts using untargeted LC-qTOF-MS/MS analysis. While the metabolomes of *PtAADC1*-expressing plants did not significantly differ from those of control plants, expression of *PtAAS1* resulted in the accumulation of phenylacetic acid (PAA) and PAA-amino acid conjugates, identified as PAA-aspartate and PAA-glutamate. Moreover, targeted LC-MS/MS analysis showed that *PtAAS1*-expressing plants accumulated significant amounts of free PAA. The measurement of PAA and PAA-Asp in undamaged and herbivory-damaged poplar leaves revealed significantly induced accumulation of PAA-Asp while levels of free PAA remained unaltered by herbivore treatment. Sequence comparisons and transcriptome analysis showed that members of a small gene family comprising five putative auxin-amido synthetase *GH3* genes potentially involved in the

48 conjugation of auxins like PAA with amino acids were significantly upregulated upon herbivory in *P.*  
49 *trichocarpa* leaves. Overall, our data indicates that phenylacetaldehyde generated by poplar PtAAS1  
50 serves as a hub metabolite linking the biosynthesis of volatile, non-volatile herbivory-induced  
51 specialized metabolites, and phytohormones, suggesting that growth and defense are balanced on a  
52 metabolic level.

53 **Keywords:** *Populus trichocarpa*, *Nicotiana benthamiana*, Auxin, aromatic amino acid synthase,  
54 *Lymantria dispar*, aromatic amino acid decarboxylase, phenylacetic acid, indole-3-acetic acid,  
55 phenylacetaldehyde, PAA-Asp, PAA-Glu.

## 56 Introduction

57 Plant specialized metabolites mediate plant responses to different biotic conditions and are  
58 generated by a plethora of biosynthetic pathways. These pathways can be initiated by key enzymes  
59 like cytochrome P450 enzymes (Irmisch et al., 2013; Sørensen et al., 2018), aminotransferases  
60 (Wang and Maeda, 2018), and group II pyridoxal phosphate (PLP)-dependent enzymes (Facchini et  
61 al., 2000). The latter comprise decarboxylase and aldehyde synthase enzymes that are involved in  
62 the biosynthesis of aromatic amino acid-derived specialized metabolites like benzyloisoquinoline  
63 alkaloids (Facchini et al., 2000), monoterpene indole alkaloids (O'Connor and Maresh, 2006),  
64 hydroxy cinnamic acid amides (Facchini et al., 2002), and phenylpropanoids in plants  
65 (Torrens-spence et al., 2018; Günther et al., 2019). For example, poplar trees under herbivore attack  
66 biosynthesize the volatile 2-phenylethanol and its glucoside 2-phenylethyl- $\beta$ -D-glucopyranoside via  
67 separate biosynthetic pathways (Günther et al., 2019). The formation of these metabolites can be  
68 initiated by the closely related group II PLP-dependent enzymes, PtAAS1 and PtAADC1. The direct  
69 reaction products of AAS and AADC enzymatic reactions phenylacetaldehyde and  
70 2-phenylethylamine have been shown to contribute to the biosynthesis of different plant metabolites,  
71 respectively (Sekimoto et al., 1998; Facchini et al., 2000; Facchini et al., 2002; Torrens-spence et al.,  
72 2018). Previously, it has been shown that 2-phenylethylamine could be transformed to  
73 phenylacetaldehyde in subsequent biosynthetic steps in planta (Boatright et al., 2004; Tieman et al.,  
74 2006). The aromatic aldehyde phenylacetaldehyde has further been proposed to contribute to the  
75 biosynthesis of the auxin phenylacetic acid (Cook and Ross, 2016; Cook et al., 2016).

76 Auxins are plant hormones of paramount impact on plant development and growth. Although  
77 indole-3-acetic acid (IAA) is the most studied amongst this group of phytohormones, other natural  
78 auxins like phenylacetic acid (PAA), indole-3-butyric acid, indole-3-propionic acid and  
79 4-chloroindole-3-acetic acid have been discovered (Abe et al., 1974; Fries and Iwasaki, 1976;  
80 Ludwig-Müller, 2011; Simon and Petrášek, 2011). Recent progress has led to an increased interest in  
81 the biosynthesis and physiology of the auxin PAA (Enders and Strader, 2016; Zhao, 2018). In  
82 comparison, IAA and PAA show distinctly different characteristics concerning their transport and  
83 distribution within the plant (Sugawara et al., 2015; Aoi et al., 2020). Both auxins target similar  
84 responsive elements, whereas a lower concentration of IAA in comparison to the concentration of  
85 PAA is sufficient to trigger these responses (Wightman and Lighty, 1982; Simon and Petrášek, 2011).  
86 Cellular concentrations of auxins are variable, and their developmental output is highly dependent on  
87 the local biosynthesis and local concentrations of these auxins (Wang et al., 2015; Zheng et al.,  
88 2016). Free auxin concentrations can be rapidly altered by auxin-amido synthetase Gretchen Hagen  
89 3 (GH3) enzymes (Westfall et al., 2016). These enzymes belong to a large family of auxin amino acid  
90 synthetases that accept IAA as well as PAA and conjugate these substrates with different amino  
91 acids (Staswick et al., 2005; Sugawara et al., 2015). Conjugation has been shown to interfere with  
92 both signaling and transport of free auxins and thereby modulate signaling in plant development  
93 (Ljung et al., 2002; Ludwig-Müller, 2011; Zheng et al., 2016). Furthermore, specific fluctuations in  
94 auxin biosynthesis and transport trigger different developmental changes in the context of adaptation  
95 to stress (Grieneisen et al., 2007; Brumos et al., 2018; Zhao, 2018; Blakeslee et al., 2019). Generally,  
96 auxins like IAA and PAA can be biosynthesized via separate biosynthetic pathways within the plant  
97 kingdom (Pollmann et al., 2006; Mano and Nemoto, 2012; Zhao, 2014; Cook and Ross, 2016). To  
98 date, much is known about the biosynthetic pathways leading to the formation of IAA in *Arabidopsis*  
99 *thaliana* (Mashiguchi et al., 2011; Zhao, 2014; Enders and Strader, 2016). Initial steps of this

100 biosynthetic network comprise the formation of indole-3-acetaldehyde and tryptamine (Supplemental  
101 Figure 1; reviewed in (Mano and Nemoto, 2012; Zhao, 2014)). In further biosynthetic steps, these  
102 intermediates can be converted to the corresponding auxin IAA. Similarly, the biosynthesis of PAA  
103 can be initiated by separate pathways leading to the formation phenylacetaldehyde (Kaminaga et al.,  
104 2006; Gutensohn et al., 2011; Günther et al., 2019) and 2-phenylethylamine (Tiemann et al., 2006;  
105 Günther et al., 2019). In subsequent biosynthetic steps, these pathways might ultimately lead to the  
106 formation of PAA (Supplemental Figure 2; (Sekimoto et al., 1998)).

107 In this study, we show that the key enzyme for generation of the herbivory-induced metabolites  
108 phenylacetaldehyde, 2-phenylethanol and 2-phenylethyl- $\beta$ -D-glucopyranoside in poplar lead to  
109 stimulated biosynthesis of the auxin PAA as well as PAA conjugates *in planta*.

## 110 Results and Discussion

### 111 Expression of *PtAAS1* and *PtAADC1* alters the accumulation of phenolic metabolites in *N.* 112 *benthamiana*

113 We expressed *PtAAS1* and *PtAADC1* in leaves of *N. benthamiana* and quantified the aromatic  
114 amino acid substrates and aromatic amine products of AADC1 as well as the indirect reaction product  
115 of AAS1, 2-phenylethyl- $\beta$ -D-glucopyranoside, via LC-MS/MS. As previously shown, levels of aromatic  
116 amines (Supplemental Figure 3) and 2-phenylethyl- $\beta$ -D-glucopyranoside (Supplemental Figure 4)  
117 were increased upon *PtAADC1* and *PtAAS1* expression, respectively (Günther et al., 2019).

118 To investigate other potential metabolic alterations in *PtAAS1*- and *PtAADC1*-expressing *N.*  
119 *benthamiana* leaves, we performed untargeted LC-qTOF-MS/MS analysis. The expression of  
120 *PtAAS1* and *PtAADC1* resulted in different metabolite profiles in comparison to wild type and  
121 eGFP-expressing control plants (Figure 1; Supplemental Table 1). The expression of *PtAAS1* and  
122 *PtAADC1* resulted in the differential accumulation of metabolites with a higher number of significantly  
123 up- or downregulated metabolites in the *PtAAS1*-expressing plants (Figure 1). Two candidate  
124 metabolites were exclusively present in *PtAAS1*-expressing lines and were identified as conjugates of  
125 phenylacetic acid with aspartate (PAA-Asp) and glutamate (PAA-Glu) via LC-qTOF-MS/MS (Figure  
126 1). Several other phenolic compounds were detected but could not be identified based on the  
127 fragmentation pattern (Supplemental Table 1).

128 Expression of *PtAAS1* and the concomitant accumulation of auxin-conjugates pointed towards a  
129 conversion of the *PtAAS1* reaction product phenylacetaldehyde to PAA-Asp and PAA-Glu in further  
130 metabolic steps in a heterologous plant system. It has been shown recently that aromatic aldehyde  
131 synthases generate aldehydes from corresponding aromatic amino acids and thereby initiate to the  
132 formation of aromatic alcohols and alcohol glucosides (Torrens-Spence et al., 2018; Günther et al.,  
133 2019). Additionally, it has been suggested that aromatic aldehydes might also contribute to the  
134 formation of plant auxins (Sekimoto et al., 1998).

135 In addition to the accumulation of 2-phenylethyl- $\beta$ -D-glucopyranoside, *PtAAS1*-expressing *N.*  
136 *benthamiana* plants also accumulated the auxin PAA in leaves (Figure 2). In comparison to reports in  
137 *Arabidopsis thaliana* rosette leaves, which were shown to contain up to 500 pmol/g fresh weight  
138 (~70ng/g fresh weight) of endogenous PAA (Sugawara et al., 2015), the amounts of up to 700 ng/g  
139 fresh weight in leaves of *PtAAS1*-expressing *N. benthamiana* plants (Figure 2) are unphysiologically  
140 high. These high concentration of the indirect *PtAAS1* product PAA might have allowed highly  
141 promiscuous endogenous enzymes to accept this metabolite as a substrate (Moghe and Last, 2015).  
142 Such enzymes might be employed for detoxification of toxic intermediates within specialized  
143 metabolism (Sirikantaramas et al., 2008). Indeed, plant auxins can be inactivated or detoxified via  
144 esterification with amino acids (Woodward and Bartel, 2005; Korasick et al., 2013). Nevertheless, our  
145 results in *N. benthamiana* illustrate that *PtAAS1* activity can lead to the formation of the  
146 phenylalanine-derived auxin PAA in a heterologous plant system.

### 147 Expression of phenylacetaldehyde-generating *PtAAS1* leads to the accumulation of PAA- and 148 IAA-conjugates in *N. benthamiana*

149 We further investigated the accumulation of PtAAS1-derived auxin metabolites in different tissues of  
150 *N. benthamiana* plants expressing PtAAS1. In order to further characterize the function of PtAAS1  
151 and PtAAD1 we developed targeted analyses to quantify the reaction products and the auxin  
152 derivatives.

153 The auxin conjugates PAA-Asp and PAA-Glu accumulated in leaves and shoots (Figure 2).  
154 Furthermore, we detected these auxin conjugates in roots, however, their levels in roots were not  
155 significantly increased in PtAAS1-expressing plants in comparison to wild type and eGFP-expression  
156 control plants (Supplemental Figure 5). It has been reported that *A. thaliana* plants with an increased  
157 PAA biosynthesis also showed an increased accumulation of PAA-Asp, PAA-Glu and IAA-aspartate  
158 conjugate (IAA-Asp; (Aoi et al., 2020)). In line with these findings, we measured significantly  
159 increased levels of IAA-Asp in leaves and shoots of PtAAS1-expressing plants (Supplemental Figure  
160 6), highlighting that the increased auxin biosynthesis is accompanied by increased conversion of both  
161 auxins IAA and PAA into their respective conjugates (Mashiguchi et al., 2011; Sugawara et al., 2015;  
162 Aoi et al., 2020). Auxin conjugation with amino acids occurs in plant tissue upon the increase of auxin  
163 biosynthesis or accumulation (Ludwig-Müller, 2011) and regulates the concentration of free, active  
164 auxin, to mitigate the developmental effects of increased auxin biosynthesis (Zhao et al., 2001;  
165 Mashiguchi et al., 2011; Bunney et al., 2017).

166 We identified that PtAAS1 contributes to the formation of the auxin PAA and its conjugates  
167 PAA-Asp and PAA-Glu in *N. benthamiana* leaves (Figure 1; 2). It has been shown recently that  
168 expression of CYP79A2 resulted in similar increase of PAA, PAA-Asp and PAA-Glu in Arabidopsis  
169 (Aoi et al., 2020). Our results indicate that the expression of PtAAS1 in *N. benthamiana* results in the  
170 increased biosynthesis of PAA and confirms the results of Aoi and colleagues that levels of other  
171 active auxins might be reduced within the plant by means of conjugation of the active forms to the  
172 inactive conjugates (Aoi et al., 2020). Furthermore, we could show that the PAA conjugates  
173 accumulate in the leaf tissue as well as in adjacent shoot and root tissue (Figure 2; Supplemental  
174 Figure 5). These results allow for speculation of a directional transport of PAA conjugates that were  
175 biosynthesized in the leaves as reviewed recently (Leyser, 2018).

176 Plant auxins are involved in various stages of plant development and defense (Grieneisen et al.,  
177 2007; Brumos et al., 2018; Günther et al., 2018; Zhao, 2018; Blakeslee et al., 2019). Local auxin  
178 concentration is strictly regulated within plants by means of transport, degradation and conjugation  
179 (Ljung et al., 2002; Staswick et al., 2005; Ludwig-Müller, 2011; Korasick et al., 2013; Sugawara et al.,  
180 2015; Zheng et al., 2016) and external application of auxins results in the increased accumulation of  
181 auxin conjugates. In this study, we induced high accumulation of the auxin PAA in a heterologous  
182 plant system via the expression of the phenylacetaldehyde-generating PtAAS1 (Figure 1; 2). The  
183 resulting accumulation of the corresponding PAA conjugates suggests that the pool size of free  
184 auxins is strictly regulated, at least partially by conversion into inactive conjugates and possibly  
185 transport of these conjugates.

186 Taken together, PtAAS1 contributes to the formation of PAA and PAA conjugates *in planta*.  
187 Additionally, as we also detected increased levels of IAA-Asp, our results provide additional evidence  
188 for the recently described crosstalk of PAA with IAA through coordinated conjugation of both free  
189 auxins (Aoi et al., 2020).

## 190 **The auxin conjugate PAA-Asp and putative GH3 transcripts accumulate in herbivory-induced** 191 **poplar leaves**

192 We next tested whether herbivory-induced *P. trichocarpa* leaves with increased PtAAS1  
193 transcript levels show accumulation of PAA and PAA-Asp. We incubated *P. trichocarpa* trees with the  
194 herbivore *Lymantria dispar* caterpillars and quantified PAA and PAA-Asp in the leaves. Notably, the  
195 accumulation of PAA was unaltered in comparison to control leaves, whereas PAA-Asp was  
196 significantly increased upon herbivory (Figure 3).

197 It has been previously shown that increased auxin biosynthesis can be accompanied by the  
198 stimulated expression of auxin responsive elements like *GH3* and *Aux/IAA* genes as well as the  
199 reduction of *SAUR* gene expression (Hagen and Guilfoyle, 2002). To evaluate whether transcripts of  
200 these gene families are upregulated in *P. trichocarpa* leaves challenged by herbivorous enemies, we  
201 screened for putative *Aux/IAA*, *GH3* and *SAUR* genes in our in-house transcriptome dataset.

202 Amongst the family of 14 *GH3* genes identified in the poplar transcriptome, five candidates were  
203 significantly induced in response to herbivory (Figure 3). Phylogenetic relationships of these  
204 herbivory-induced transcript suggests that these genes might indeed encode GH3 enzymes that  
205 catalyze the conjugation of the auxin PAA with amino acids (Supplemental Figure 7; (Staswick et al.,  
206 2005; Böttcher et al., 2011; Peat et al., 2012; Yu et al., 2018)). The *Aux/IAA* gene family in poplar  
207 consists of 15 putative members, two of which were significantly upregulated in herbivory-induced  
208 poplar leaves (Supplemental Figure 8). No transcripts of the 104-membered putative *SAUR* gene  
209 family were differentially expressed (Supplemental Table 2). These results suggest that upon  
210 herbivory, putative *GH3* transcripts accumulate in poplar. The corresponding GH3 enzymes might  
211 lead to the formation of PAA-Asp in herbivory-induced poplar leaves. At the time of harvest, 24 hours  
212 after the start of the herbivore treatment, the PAA concentration had most likely returned to basal  
213 levels, whereas the level of the conjugation product was still increased.

214 Taken together, our results highlight a potential unprecedented role of PtAAS1 in the biosynthesis of  
215 the auxin PAA *in planta*. We hypothesize that the expression of *PtAAS1* in *N. benthamiana* leaves  
216 leads to an increased metabolic flow to generate high amounts of volatile 2-phenylethanol,  
217 2-phenylethyl- $\beta$ -D-glucopyranoside (Günther et al., 2019), PAA and PAA-conjugates in response to  
218 an increased biosynthesis of the hub metabolite phenylacetaldehyde. As suggested recently, plant  
219 specialized metabolites might be integrated into regulation of plant signaling, growth and  
220 development (Erb and Kliebenstein, 2020).

221 Several studies revealed that the expression of key biosynthetic enzymes that initiate the  
222 biosynthesis of aromatic amino acid-derived specialized metabolites resulted in altered auxin  
223 phenotypes and chemotypes (Bak and Feyereisen, 2001; Bak et al., 2001; Irmisch et al., 2015;  
224 Günther et al., 2018; Perez et al., 2021; Perez et al., 2022). In Arabidopsis, another link between  
225 specialized metabolism and auxin signaling might be established by indole glucosinolate hydrolysis  
226 products with high affinity to the major auxin receptor Transport Inhibitor Response 1 (TIR1), which  
227 could result in competitive binding and thereby feed into the auxin signaling cascade (Vik et al., 2018).  
228 Therefore, it may not only be auxin itself but also structural analogues like indole glucosinolates and  
229 their hydrolysis products that trigger auxin-induced developmental effects. Additionally, it has been  
230 recently reported, that other non-aromatic glucosinolate catabolites are able to stimulate auxin-like  
231 phenotypes in Arabidopsis roots (Katz et al., 2015; Katz et al., 2020). Similarly, the maize defense  
232 compounds benzoxazolinones might contribute to auxin-induced growth through the interference with  
233 auxin perception (Hoshi-Sakoda et al., 1994), as maize CYP79A enzymes contribute to the formation  
234 of phenylalanine-derived defense compounds as well as to the formation of the corresponding auxin  
235 PAA in a heterologous plant system (Irmisch et al., 2015). Finally, the most recent study of Aoi and  
236 colleagues showed that the expression of *CYP79A2* that leads to the formation of  
237 (*E/Z*)-phenylacetaldoxime in Arabidopsis resulted in effects similar to those of increased auxin  
238 biosynthesis and auxin conjugation (Aoi et al., 2020). Several different pathways classified as  
239 specialized metabolism appear to have evolved to not only mediate plant biotic interaction, but also  
240 provide regulatory input to auxin signaling. Increased expression of biosynthetic enzymes involved in  
241 the biosynthesis of amino acid-derived specialized metabolites might directly influence the  
242 homeostasis of the corresponding auxins.

243 In summary, the poplar aromatic aldehyde synthase PtAAS1 contributes to the  
244 herbivory-induced formation of volatile 2-phenylethanol and 2-phenylethyl- $\beta$ -D-glucopyranoside and  
245 additionally to the formation of the auxin PAA and auxin-derived conjugates in a heterologous plant  
246 system. We show that the conjugate of PAA-Asp accumulates upon herbivory in poplar leaves,  
247 suggesting that herbivory-induced expression of *PtAAS1* might contribute to PAA biosynthesis and  
248 might stimulate PAA signaling and metabolism in poplar. We conclude that the biosynthesis of the  
249 hub metabolite phenylacetaldehyde is of paramount importance for the generation of the auxin PAA  
250 and represents an additional pathway for the formation of the auxin PAA, expanding the metabolic  
251 network of the convergent biosynthesis of this auxin *in planta* (Figure 4). We unraveled  
252 unprecedented aspects of the biosynthesis of the auxin PAA in a heterologous plant system as well  
253 as in response to herbivory in *P. trichocarpa* leaves. Therefore, the phenylacetaldehyde hub  
254 metabolite represents a metabolic link between volatile, non-volatile herbivory-induced specialized  
255 metabolites, and phytohormones, suggesting that both growth and defense are balanced on a

256 metabolic level. Further research needs to be aimed at elucidating and understanding the plant  
257 physiological responses following the increased PAA biosynthesis and conjugation upon herbivory.

## 258 **Materials and Methods**

### 259 **Plant material and treatment**

260 *Populus trichocarpa* (genotype Muhle Larsen) trees were grown, *Lymantria dispar* herbivory was  
261 induced and all leaves (including midrib) and shoots (stem and petiole) were harvested. Roots were  
262 cleared of soil by washing in a fresh water bath, dried with a paper towel. All plant samples were  
263 frozen in liquid nitrogen immediately after harvesting. Plant samples were stored at -80 °C until further  
264 processing as described earlier (Günther et al., 2019). Agrobacterium-mediated expression of target  
265 genes in *N. benthamiana* was performed as described (Günther et al., 2019). Three days after  
266 transformation, plants were placed under mild direct light (LED 40%) for three more days.

### 267 **LC-qTOF-MS/MS analysis of *N. benthamiana* methanol extracts**

268 Methanol extracts (10:1 v/w) of *N. benthamiana* leaves were analyzed on an Ultimate 3000 UHPLC  
269 equipped with an Acclaim column (150 mm × 2.1 mm, particle size 2.2 µm) and connected to an  
270 IMPACT II UHR-Q-TOF-MS system (Bruker Daltonics) following a previously described program in  
271 positive and negative ionization mode (He et al., 2019). Raw data files were analyzed using Bruker  
272 Compass DataAnalysis software version 4.3. Metabolomic differences of extracts were analyzed via  
273 MetaboScape 4.0 (Supplemental Table 1). Furthermore, untargeted MS/MS data was normalized  
274 and visualized in volcano plots via XCMS (Tautenhahn et al., 2012; Gowda et al., 2014; Rinehart et  
275 al., 2014; Benton et al., 2015; Johnson et al., 2016).

### 276 **LC-MS/MS analysis of plant methanol extracts**

277 Metabolites were extracted from ground plant material (*P. trichocarpa* or *N. benthamiana*) with  
278 methanol (10:1 v/w). Analytes were separated using an Agilent 1200 HPLC system on a Zorbax  
279 Eclipse XDB-C18 column (5034.6 mm, 1.8 µm; Agilent Technologies). HPLC parameters are given in  
280 Supplemental Table 3. The HPLC was coupled to an API-6500 tandem mass spectrometer (Sciex)  
281 equipped with a turbospray ion source (ion spray voltage, 4500 eV; turbo gas temperature, 700 °C;  
282 nebulizing gas, 60 p.s.i.; curtain gas, 40 p.s.i.; heating gas, 60 p.s.i.; collision gas, 2 p.s.i.). Multiple  
283 reaction monitoring (MRM) was used to monitor a parent ion → product ion reactions given in  
284 Supplemental Table 4. The identification of PAA and IAA conjugates was performed according to  
285 LC-MS/MS fragmentation patterns as described in (Irmisch et al., 2013; Sugawara et al., 2015;  
286 Westfall et al., 2016; Günther et al., 2018; Günther et al., 2019). Relative quantification was based on  
287 the relative abundance in measured extracts based on counts per second in standardized  
288 measurement conditions. Identification and quantification of PAA, 2-phenylethylamine, tyramine,  
289 tryptamine, 2-phenylethyl-β-D-glucopyranoside, tyrosine, tryptophan and phenylalanine was  
290 performed with authentic, commercially available standards (Supplemental Table 5).

### 291 **Statistics**

292 Statistical analysis was carried out as described in the figure legends. Student's t tests,  
293 Mann-Whitney Rank Sum tests, Kruskal-Wallis one-way analysis of variance (ANOVA), Dunn's tests  
294 and Tukey tests were performed with the software SigmaPlot 14.0 (Systat Software). EDGE tests for  
295 analysis of RNA-Seq datasets were performed with CLC Genomics Workbench (Qiagen Informatics)  
296 as described earlier (Günther et al., 2019).

### 297 **RNA extraction, cDNA synthesis and RNA-Seq analysis**

298 Poplar leaf RNA extraction, cDNA synthesis and RNA-Seq analysis were carried out as  
299 described (Günther et al., 2019). For the identification of putative *Aux/IAA*, *GH3* and *SAUR* genes in  
300 the *P. trichocarpa* genome (Tuskan et al., 2006), the transcriptome annotations as mapped to the

301 poplar gene model version 3.0 provided by Phytozome (<https://phytozome.jgi.doe.gov/pz/portal.html>)  
302 were used for identification of members of the *Aux/IAA*, *GH3* and *SAUR* gene families. Candidates of  
303 the *Aux/IAA* and *GH3* gene family identified as herbivory-induced with above average fold change  
304 and p-values below  $P = 0.05$  were selected for visualization (Figure 3; Supplemental Figure 9;  
305 Supplemental Table 2). Total RPKM counts of all control and all herbivore-induced treatments were  
306 summed for the estimate of total transcript differences within the *SAUR* gene expression  
307 (Supplemental Table 2).

### 308 **Phylogenetic analysis**

309 Evolutionary analyses were conducted in MEGA X (Kumar et al., 2018)(Kumar et al., 2018).  
310 Coding sequences were retrieved from Phytozome (<https://phytozome.jgi.doe.gov/pz/portal.html>)  
311 and a multiple codon sequence alignment was performed via the guidance 2 server (Landan and  
312 Graur, 2008; Penn et al., 2010; Sela et al., 2015). The evolutionary history was inferred by using the  
313 Maximum Likelihood method based on the General Time Reversible model (Nei and Kumar, 2000).  
314 Initial trees were obtained automatically by applying Neighbor-Join and BioNJ algorithms to a matrix  
315 of pairwise distances estimated using the Maximum Composite Likelihood (MCL) approach, and then  
316 selecting the topology with superior log likelihood value. A discrete Gamma distribution was used to  
317 model evolutionary rate differences among sites (5 categories (+G, parameter = 1.5416)). The rate  
318 variation model allowed for sites to be evolutionarily invariable ([+I], 13.41% sites).

### 319 **References**

- 320 **Abe, H., Uchiyama, M., and Sato, R.** (1974). Isolation of phenylacetic acid and its p>-hydroxy derivative as  
321 auxin-like substances from undaria pinnatifida. *Agric. Biol. Chem.* **38**:897–898.
- 322 **Aoi, Y., Tanaka, K., Cook, S. D., Hayashi, K. I., and Kasahara, H.** (2020). GH3 auxin-amido synthetases alter  
323 the ratio of indole-3-acetic acid and phenylacetic acid in Arabidopsis. *Plant Cell Physiol.* **61**:596–605.
- 324 **Bak, S., and Feyereisen, R.** (2001). The Involvement of Two P450 Enzymes, CYP83B1 and CYP83A1, in Auxin  
325 Homeostasis and Glucosinolate Biosynthesis. *Plant Physiol.* **127**:108–118.
- 326 **Bak, S., Tax, F. E., Feldmann, K. A., Galbraith, D. W., and Feyereisen, R.** (2001). CYP83B1, a Cytochrome  
327 P450 at the Metabolic Branch Point in Auxin and Indole Glucosinolate Biosynthesis in Arabidopsis. *Plant*  
328 *Cell Online* **13**:101–111.
- 329 **Benton, H. P., Ivanisevic, J., Mahieu, N. G., Kurczyk, M. E., Johnson, C. H., Franco, L., Rinehart, D.,  
330 Valentine, E., Gowda, H., Ubhi, B. K., et al.** (2015). Autonomous metabolomics for rapid metabolite  
331 identification in global profiling. *Anal. Chem.* **87**:884–891.
- 332 **Blakeslee, J. J., Spatola Rossi, T., Kriechbaumer, V., and Raines, C.** (2019). Auxin biosynthesis: Spatial  
333 regulation and adaptation to stress. *J. Exp. Bot.* **70**:5041–5049.
- 334 **Boatright, J., Negre, F., Chen, X., Kish, C. M., Wood, B., Peel, G., Orlova, I., Gang, D., Rhodes, D., and  
335 Dudareva, N.** (2004). Understanding in Vivo Benzenoid Metabolism in Petunia Petal Tissue. *Plant Physiol.*  
336 **135**:1993–2011.
- 337 **Böttcher, C., Boss, P. K., and Davies, C.** (2011). Acyl substrate preferences of an IAA-amido synthetase  
338 account for variations in grape (*Vitis vinifera* L.) berry ripening caused by different auxinic compounds  
339 indicating the importance of auxin conjugation in plant development. *J. Exp. Bot.* **62**:4267–4280.
- 340 **Brumos, J., Robles, L. M., Yun, J., Vu, T. C., Jackson, S., Alonso, J. M., Stepanova, A. N., Brumos, J.,  
341 Robles, L. M., Yun, J., et al.** (2018). Local Auxin Biosynthesis Is a Key Regulator of Plant Article Local  
342 Auxin Biosynthesis Is a Key Regulator of Plant Development. *Dev. Cell* **47**:306-318.e5.
- 343 **Bunney, P. E., Zink, A. N., Holm, A. A., Billington, C. J., and Kotz, C. M.** (2017). Local auxin metabolism  
344 regulates environment-induced hypocotyl elongation. *Physiol. Behav.* **176**:139–148.
- 345 **Cook, S. D., and Ross, J. J.** (2016). The auxins, IAA and PAA, are synthesized by similar steps catalyzed by

- 346 different enzymes. *Plant Signal. Behav.* **11**:1–4.
- 347 **Cook, S. D., Nichols, D. S., Smith, J., Chourey, P. S., McAdam, E. L., Quittenden, L., and Ross, J. J.**
- 348 (2016). Auxin Biosynthesis: Are the Indole-3-Acetic Acid and Phenylacetic Acid Biosynthesis Pathways
- 349 Mirror Images? *Plant Physiol.* **171**:1230–41.
- 350 **Enders, T. A., and Strader, L. C.** (2016). Auxin Activity: Past, present, and Future. *Am. J. Bot.* **102**:180–196.
- 351 **Erb, M., and Kliebenstein, D. J.** (2020). Plant Secondary Metabolites as Defenses, Regulators, and Primary
- 352 Metabolites: The Blurred Functional Trichotomy1[OPEN]. *Plant Physiol.* **184**:39–52.
- 353 **Facchini, P. J., Huber-Allanach, K. L., and Tari, L. W.** (2000). Plant aromatic L-amino acid decarboxylases:
- 354 Evolution, biochemistry, regulation, and metabolic engineering applications. *Phytochemistry* **54**:121–138.
- 355 **Facchini, P. J., Hagel, J., and Zulak, K. G.** (2002). Hydroxycinnamic acid amide metabolism: physiology and
- 356 biochemistry. *Can. J. Bot.* **80**:577–589.
- 357 **Fries, L., and Iwasaki, H.** (1976). p-Hydroxyphenylacetic acid and other phenolic compounds as growth
- 358 stimulators of the red alga *Porphyra tenera*. *Plant Sci. Lett.* **6**:299–307.
- 359 **Gowda, H., Ivanisevic, J., Johnson, C. H., Kurczy, M. E., Benton, H. P., Rinehart, D., Nguyen, T., Ray, J.,**
- 360 **Kuehl, J., Arevalo, B., et al.** (2014). Interactive XCMS online: Simplifying advanced metabolomic data
- 361 processing and subsequent statistical analyses. *Anal. Chem.* **86**:6931–6939.
- 362 **Grieneisen, V. A., Xu, J., Marée, A. F. M., Hogeweg, P., and Scheres, B.** (2007). Auxin transport is sufficient
- 363 to generate a maximum and gradient guiding root growth. *Nature* **449**:1008–1013.
- 364 **Günther, J., Irmisch, S., Lackus, N. D., Reichelt, M., Gershenzon, J., and Köllner, T. G.** (2018). The nitrilase
- 365 PtNIT1 catabolizes herbivore-induced nitriles in *Populus trichocarpa*. *BMC Plant Biol.* **18**:1–12.
- 366 **Günther, J., Lackus, N. D., Schmidt, A., Huber, M., Stödler, H.-J., Reichelt, M., Gershenzon, J., and**
- 367 **Köllner, T. G.** (2019). Separate pathways contribute to the herbivore-induced formation of
- 368 2-phenylethanol in poplar. *Plant Physiol.* **180**:767–782.
- 369 **Gutensohn, M., Klempien, A., Kaminaga, Y., Nagegowda, D. A., Negre-Zakharov, F., Huh, J. H., Luo, H.,**
- 370 **Weizbauer, R., Mengiste, T., Tholl, D., et al.** (2011). Role of aromatic aldehyde synthase in
- 371 wounding/herbivory response and flower scent production in different *Arabidopsis* ecotypes. *Plant J.*
- 372 **66**:591–602.
- 373 **Hagen, G., and Guilfoyle, T.** (2002). Auxin-responsive gene expression: genes, promoters and regulatory
- 374 factors. *Plant Mol. Biol.* **49**:373–385.
- 375 **He, J., Fandino, R. A., Halitschke, R., Luck, K., Köllner, T. G., Murdock, M. H., Ray, R., Gase, K., Knaden,**
- 376 **M., Baldwin, I. T., et al.** (2019). An unbiased approach elucidates variation in (S)-(+)-linalool, a
- 377 context-specific mediator of a tri-trophic interaction in wild tobacco. *Proc. Natl. Acad. Sci. U. S. A.*
- 378 **116**:14651–14660.
- 379 **Hoshi-Sakoda, M., Usui, K., Ishizuka, K., Kosemura, S., Yamamura, S., and Hasegawa, K.** (1994).
- 380 Structure-activity relationships of benzoxazolinones with respect to auxin-induced growth and
- 381 auxin-binding protein. *Phytochemistry* **37**:297–300.
- 382 **Irmisch, S., Clavijo McCormick, A., Boeckler, G. A., Schmidt, A., Reichelt, M., Schneider, B., Block, K.,**
- 383 **Schnitzler, J.-P., Gershenzon, J., Unsicker, S. B., et al.** (2013). Two Herbivore-Induced Cytochrome
- 384 P450 Enzymes CYP79D6 and CYP79D7 Catalyze the Formation of Volatile Aldoximes Involved in Poplar
- 385 Defense. *Plant Cell* **25**:4737–4754.
- 386 **Irmisch, S., Zeltner, P., Handrick, V., Gershenzon, J., and Köllner, T. G.** (2015). The maize cytochrome P450
- 387 CYP79A61 produces phenylacetaldoxime and indole-3-acetaldoxime in heterologous systems and might
- 388 contribute to plant defense and auxin formation. *BMC Plant Biol.* **15**:128.
- 389 **Johnson, C. H., Ivanisevic, J., and Siuzdak, G.** (2016). Metabolomics: beyond biomarkers and towards



- 390 mechanisms. *Nat. Rev. Mol. Cell Biol.* **17**:451–459.
- 391 **Kaminaga, Y., Schnepp, J., Peel, G., Kish, C. M., Ben-Nissan, G., Weiss, D., Orlova, I., Lavie, O., Rhodes,**  
392 **D., Wood, K., et al.** (2006). Plant phenylacetaldehyde synthase is a bifunctional homotetrameric enzyme  
393 that catalyzes phenylalanine decarboxylation and oxidation. *J. Biol. Chem.* **281**:23357–23366.
- 394 **Katz, E., Nisani, S., Yadav, B. S., Woldemariam, M. G., Shai, B., Obolski, U., Ehrlich, M., Shani, E., Jander,**  
395 **G., and Chamovitz, D. A.** (2015). The glucosinolate breakdown product indole-3-carbinol acts as an auxin  
396 antagonist in roots of *Arabidopsis thaliana*. *Plant J.* **82**:547–555.
- 397 **Katz, E., Bagchi, R., Jeschke, V., Rasmussen, A. R. M., Hopper, A., Burow, M., Estelle, M., and**  
398 **Kliebenstein, D. J.** (2020). Diverse allyl glucosinolate catabolites independently influence root growth and  
399 development. *Plant Physiol.* **183**:1376–1390.
- 400 **Korasick, D. A., Enders, T. A., and Strader, L. C.** (2013). Auxin biosynthesis and storage forms. *J. Exp. Bot.*  
401 **64**:2541–2555.
- 402 **Kumar, S., Stecher, G., Li, M., Knyaz, C., and Tamura, K.** (2018). MEGA X: Molecular evolutionary genetics  
403 analysis across computing platforms. *Mol. Biol. Evol.* **35**:1547–1549.
- 404 **Landan, G., and Graur, D.** (2008). Local reliability measures from sets of co-optimal multiple sequence  
405 alignments. *Pacific Symp. Biocomput.* **13**:15–24.
- 406 **Leyser, O.** (2018). Auxin signaling. *Plant Physiol.* **176**:465–479.
- 407 **Ljung, K., Hull, A. K., Kowalczyk, M., Marchant, A., Celenza, J., Cohen, J. D., and Sandberg, G.** (2002).  
408 Biosynthesis, conjugation, catabolism and homeostasis of indole-3-acetic acid in *Arabidopsis thaliana*.  
409 *Plant Mol. Biol.* **50**:309–332.
- 410 **Ludwig-Müller, J.** (2011). Auxin conjugates: Their role for plant development and in the evolution of land plants.  
411 *J. Exp. Bot.* **62**:1757–1773.
- 412 **Mano, Y., and Nemoto, K.** (2012). The pathway of auxin biosynthesis in plants. *J. Exp. Bot.* **63**:2853–2872.
- 413 **Mashiguchi, K., Tanaka, K., Sakai, T., Sugawara, S., Kawaide, H., Natsume, M., Hanada, A., Yaeno, T.,**  
414 **Shirasu, K., Yao, H., et al.** (2011). The main auxin biosynthesis pathway in *Arabidopsis*. *Proc. Natl. Acad.*  
415 *Sci.* **108**:18512–18517.
- 416 **Moghe, G., and Last, R. L.** (2015). Something old, something new: Conserved enzymes and the evolution of  
417 novelty in plant specialized metabolism. *Plant Physiol.* **169**:pp.00994.2015.
- 418 **Nei, M., and Kumar, S.** (2000). *Molecular evolution and phylogenetics*. Oxford university press.
- 419 **O'Connor, S. E., and Maresh, J. J.** (2006). Chemistry and biology of monoterpene indole alkaloid biosynthesis.  
420 *Nat. Prod. Rep.* **23**:532–547.
- 421 **Peat, T. S., Böttcher, C., Newman, J., Lucent, D., Cowieson, N., and Davies, C.** (2012). Crystal structure of  
422 an indole-3-acetic acid amido synthetase from grapevine involved in auxin homeostasis. *Plant Cell*  
423 **24**:4525–4538.
- 424 **Penn, O., Privman, E., Ashkenazy, H., Landan, G., Graur, D., and Pupko, T.** (2010). GUIDANCE: A web  
425 server for assessing alignment confidence scores. *Nucleic Acids Res.* **38**:23–28.
- 426 **Perez, V. C., Dai, R., Bai, B., Tomiczek, B., Askey, B. C., Zhang, Y., Rubin, G. M., Ding, Y., Grenning, A.,**  
427 **Block, A. K., et al.** (2021). Aldoximes are precursors of auxins in *Arabidopsis* and maize. *New Phytol.*  
428 Advance Access published 2021, doi:10.1111/nph.17447.
- 429 **Perez, V. C., Dai, R., Tomiczek, B., Mendoza, J., Wolf, E. S. A., Grenning, A., Vermerris, W., Block, A. K.,**  
430 **and Kim, J.** (2022). Metabolic link between auxin production and specialized metabolites in *Sorghum*  
431 *bicolor* Advance Access published 2022.
- 432 **Pollmann, S., Müller, A., and Weiler, E. W.** (2006). Many roads lead to “auxin”: Of nitrilases, synthases, and  
433 amidases. *Plant Biol.* **8**:326–333.

- 434 Rinehart, D., Johnson, C. H., Nguyen, T., Ivanisevic, J., Benton, H. P., Lloyd, J., Arkin, A. P.,  
435 Deutschbauer, A. M., Patti, G. J., and Siuzdak, G. (2014). Metabolomic data streaming for  
436 biology-dependent data acquisition. *Nat. Biotechnol.* **32**:524–527.
- 437 Sekimoto, H., Seo, M., Kawakami, N., Komano, T., Desloire, S., Liotenberg, S., Marion-Poll, A., Caboche,  
438 M., Kamiya, Y., and Koshiba, T. (1998). Molecular cloning and characterization of aldehyde oxidases in  
439 *Arabidopsis thaliana*. *Plant Cell Physiol.* **39**:433–442.
- 440 Sela, I., Ashkenazy, H., Katoh, K., and Pupko, T. (2015). GUIDANCE2: Accurate detection of unreliable  
441 alignment regions accounting for the uncertainty of multiple parameters. *Nucleic Acids Res.* **43**:W7–W14.
- 442 Simon, S., and Petrášek, J. (2011). Why plants need more than one type of auxin. *Plant Sci.* **180**:454–460.
- 443 Sirikantaramas, S., Yamazaki, M., and Saito, K. (2008). Mechanisms of resistance to self-produced toxic  
444 secondary metabolites in plants. *Phytochem. Rev.* **7**:467–477.
- 445 Sørensen, M., Neilson, E. H. J., and Møller, B. L. (2018). Oximes L: Unrecognized Chameleons in General and  
446 Specialized Plant Metabolism. *Mol. Plant* **11**:95–117.
- 447 Staswick, P. E., Serban, B., Rowe, M., Tiryaki, I., Maldonado, M. T., Maldonado, M. C., and Suza, W.  
448 (2005). Characterization of an Arabidopsis Enzyme Family That Conjugates Amino Acids to  
449 Indole-3-Acetic Acid. *Plant Cell* **17**:616–627.
- 450 Sugawara, S., Mashiguchi, K., Tanaka, K., Hishiyama, S., Sakai, T., Hanada, K., Kinoshita-Tsujimura, K.,  
451 Yu, H., Dai, X., Takebayashi, Y., et al. (2015). Distinct Characteristics of Indole-3-Acetic Acid and  
452 Phenylacetic Acid, Two Common Auxins in Plants. *Plant Cell Physiol.* **56**:1641–1654.
- 453 Tautenhahn, R., Cho, K., Uritboonthai, W., Zhu, Z., Patti, G. J., and Siuzdak, G. (2012). An accelerated  
454 workflow for untargeted metabolomics using the METLIN database. *Nat. Biotechnol.* **30**:826–828.
- 455 Tieman, D., Taylor, M., Schauer, N., Fernie, A. R., Hanson, A. D., and Klee, H. J. (2006). Tomato aromatic  
456 amino acid decarboxylases participate in synthesis of the flavor volatiles 2-phenylethanol and  
457 2-phenylacetaldehyde. *Proc. Natl. Acad. Sci.* **103**:8287–8292.
- 458 Torrens-Spence, M. P., Li, F., Carballo, V., and Weng, J. (2018). Complete Pathway Elucidation and  
459 Heterologous Reconstitution of Rhodiola Salidroside Biosynthesis Advance Access published 2018,  
460 doi:10.1016/j.molp.2017.12.007.
- 461 Tuskan, G. A., DiFazio, S., Jansson, S., Bohlmann, J., Grigoriev, I., Hellsten, U., Putnam, N., Ralph, S.,  
462 Rombauts, S., Salamov, A., et al. (2006). The Genome of Black Cottonwood, *Populus trichocarpa* (Torr.  
463 & Gray). *Science (80- )*. **313**:1596–1604.
- 464 Vik, D., Mitarai, N., Wulff, N., Halkier, B. A., and Burow, M. (2018). Dynamic modeling of indole glucosinolate  
465 hydrolysis and its impact on auxin signaling. *Front. Plant Sci.* **9**:1–16.
- 466 Wang, M., and Maeda, H. A. (2018). Aromatic amino acid aminotransferases in plants. *Phytochem. Rev.*  
467 **17**:131–159.
- 468 Wang, B., Chu, J., Yu, T., Xu, Q., Sun, X., Yuan, J., Xiong, G., Wang, G., Wang, Y., and Li, J. (2015).  
469 Tryptophan-independent auxin biosynthesis contributes to early embryogenesis in *Arabidopsis*. *Proc. Natl.*  
470 *Acad. Sci.* **112**:4821–4826.
- 471 Westfall, C. S., Sherp, A. M., Zubieta, C., Alvarez, S., Schraft, E., Marcellin, R., Ramirez, L., and Jez, J. M.  
472 (2016). *Arabidopsis thaliana* GH3.5 acyl acid amido synthetase mediates metabolic crosstalk in auxin and  
473 salicylic acid homeostasis. *Proc. Natl. Acad. Sci.* **113**:13917–13922.
- 474 Wightman, F., and Lighty, D. L. (1982). Identification of phenylacetic acid as a natural auxin in the shoots of  
475 higher plants. *Physiol. Plant.* **55**:17–24.
- 476 Woodward, A. W., and Bartel, B. (2005). Auxin: Regulation, action, and interaction. *Ann. Bot.* **95**:707–735.
- 477 Yu, D., Qanmber, G., Lu, L., Wang, L., Li, J., Yang, Z., Liu, Z., Li, Y., Chen, Q., Mendu, V., et al. (2018).

478            Genome-wide analysis of cotton GH3 subfamily II reveals functional divergence in fiber development,  
479            hormone response and plant architecture. *BMC Plant Biol.* **18**.  
480 **Zhao, Y.** (2014). Auxin Biosynthesis. *Arab. B.* **12**:e0173.  
481 **Zhao, Y.** (2018). Essential Roles of Local Auxin Biosynthesis in Plant Development and in Adaptation to  
482            Environmental Changes. *Annu. Rev. Plant Biol.* **69**:417–435.  
483 **Zhao, Y., Christensen, S. K., Fankhauser, C., Cashman, J. R., Cohen, J. D., Weigel, D., and Chory, J.**  
484            (2001). A role for flavin monooxygenase-like enzymes in auxin biosynthesis. *Science (80-. )*. **291**:306–309.  
485 **Zheng, Z., Guo, Y., Novák, O., Chen, W., Ljung, K., Noel, J. P., and Chory, J.** (2016). Local auxin metabolism  
486            regulates environmentinduced hypocotyl elongation. *Nat. Plants* **2**:1–9.  
487

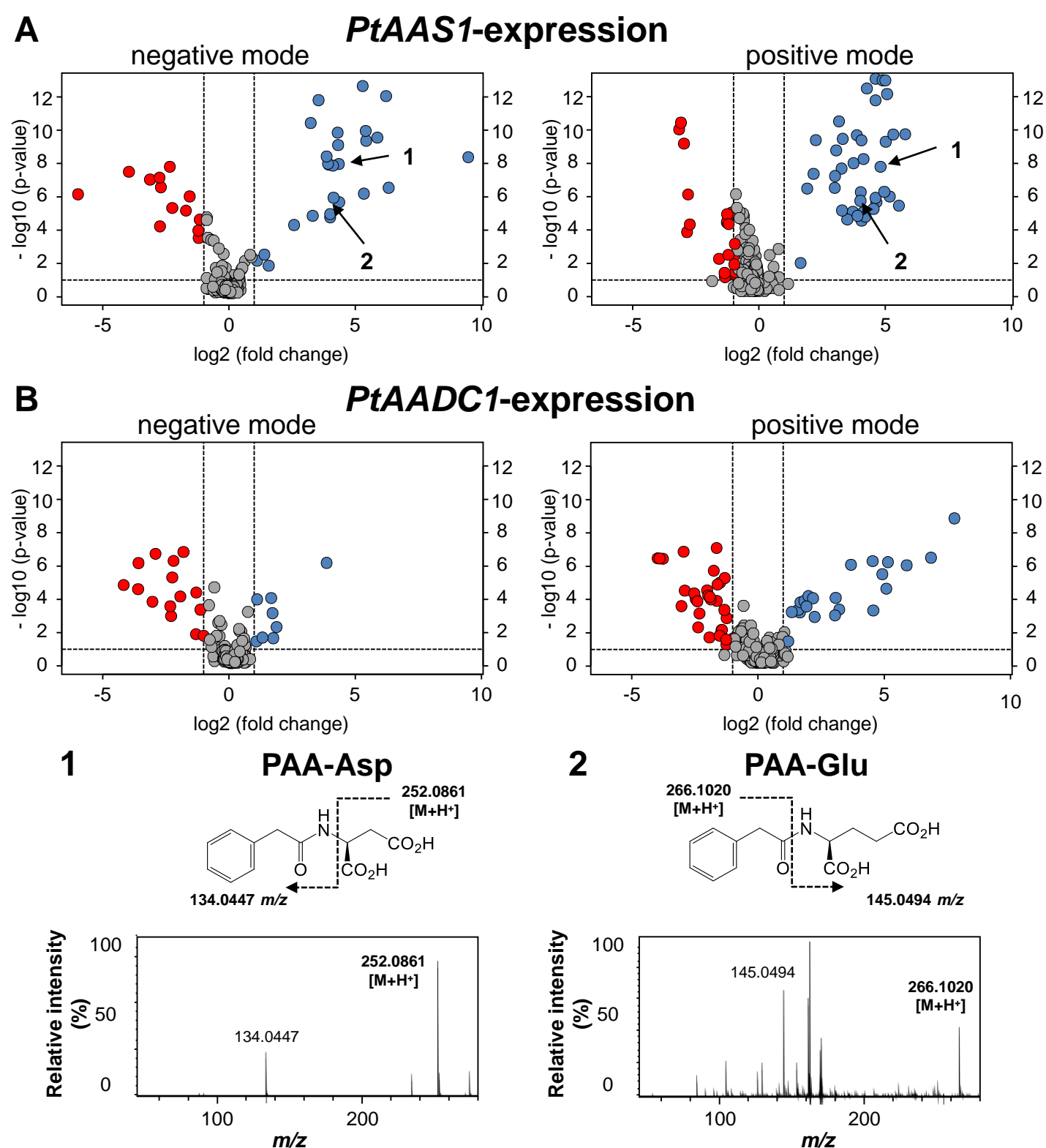


**Figure 1: Untargeted LC-qTOF-MS/MS reveals significantly altered metabolites in *PtAAS1*- and *PtAADC1*-expressing *N. benthamiana* leaves.**

Volcano plots of normalized LC-qTOF-MS/MS analysis of significantly upregulated (blue) and downregulated (red) metabolites in (A) *PtAAS1*- and (B) *PtAADC1*-expressing *N. benthamiana* plants in comparison to *eGFP*-expressing control plants (n = 6). The conjugates PAA-Asp (1) and PAA-Glu (2) could be identified only in methanol extracts of leaves of *PtAAS1*-expressing *N. benthamiana*. Mass spectra of the identified compounds PAA-Asp (1) and PAA-Glu (2) in positive ionization mode are shown.

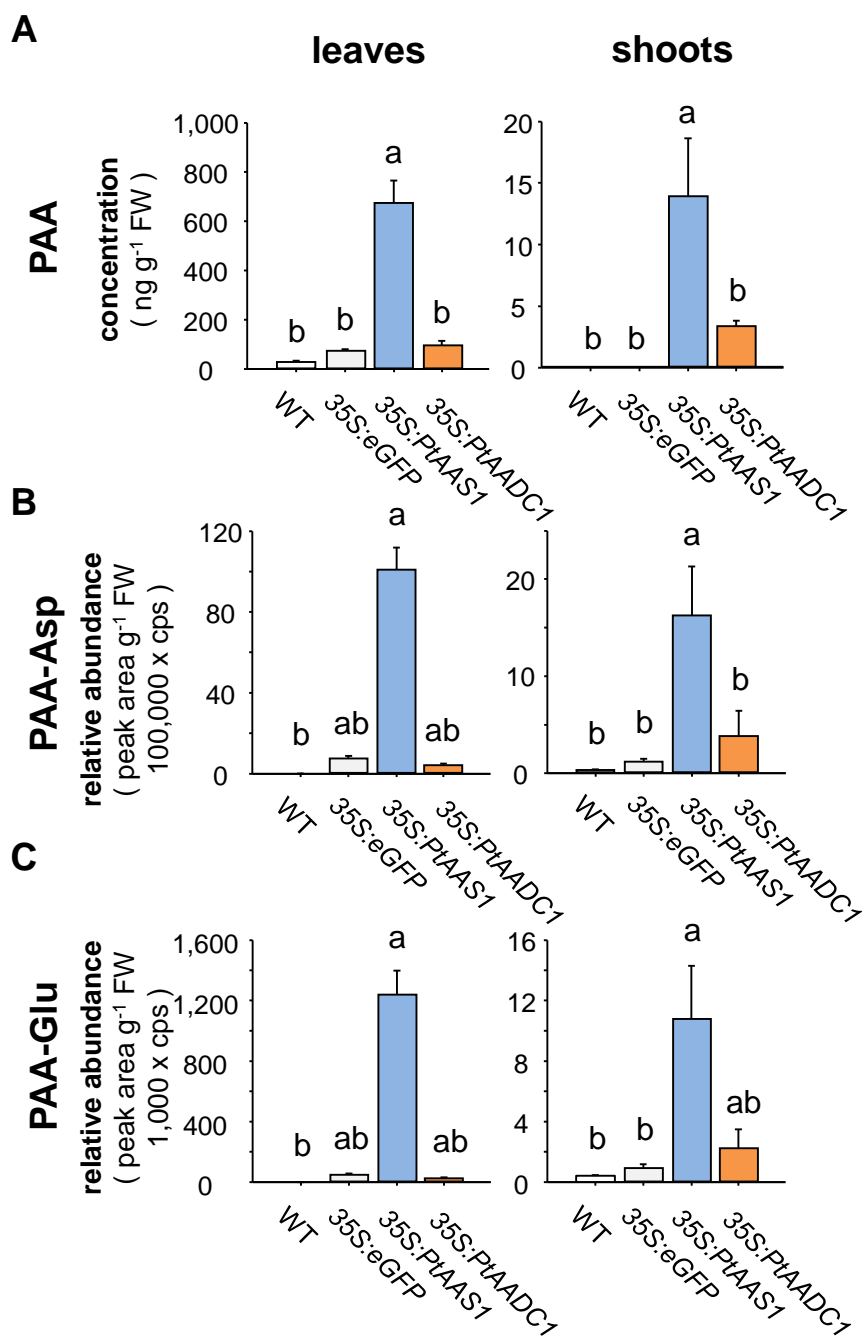


**Figure 2: Expression of *PtAAS1* results in increased levels of the auxin PAA, and its conjugates PAA-Asp and PAA-Glu in *N. benthamiana* leaves and shoots.**

*N. benthamiana* leaves expressing poplar *PtAAS1* accumulate high amounts of (A) PAA, (B) PAA-Glu and (C) PAA-Asp in leaves and shoots. Different letters above each bar indicates statistically significant differences (Kruskal-Wallis One Way ANOVA) and are based on the following Tukey (shoots) or Dunn's test (leaves): PAA<sub>leaves</sub> (H = 19.607, P ≤ 0.001); PAA<sub>shoot</sub> (H = 12.275, P = 0.006); PAA-Asp<sub>leaves</sub> (H = 20.747, P ≤ 0.001); PAA-Asp<sub>shoot</sub> (H = 19.127, P ≤ 0.001); PAA-Glu<sub>leaves</sub> (H = 19.924, P ≤ 0.001); PAA-Glu<sub>shoot</sub> (H = 15.647, P = 0.001). Means + SE are shown (n = 6). FW, fresh weight.

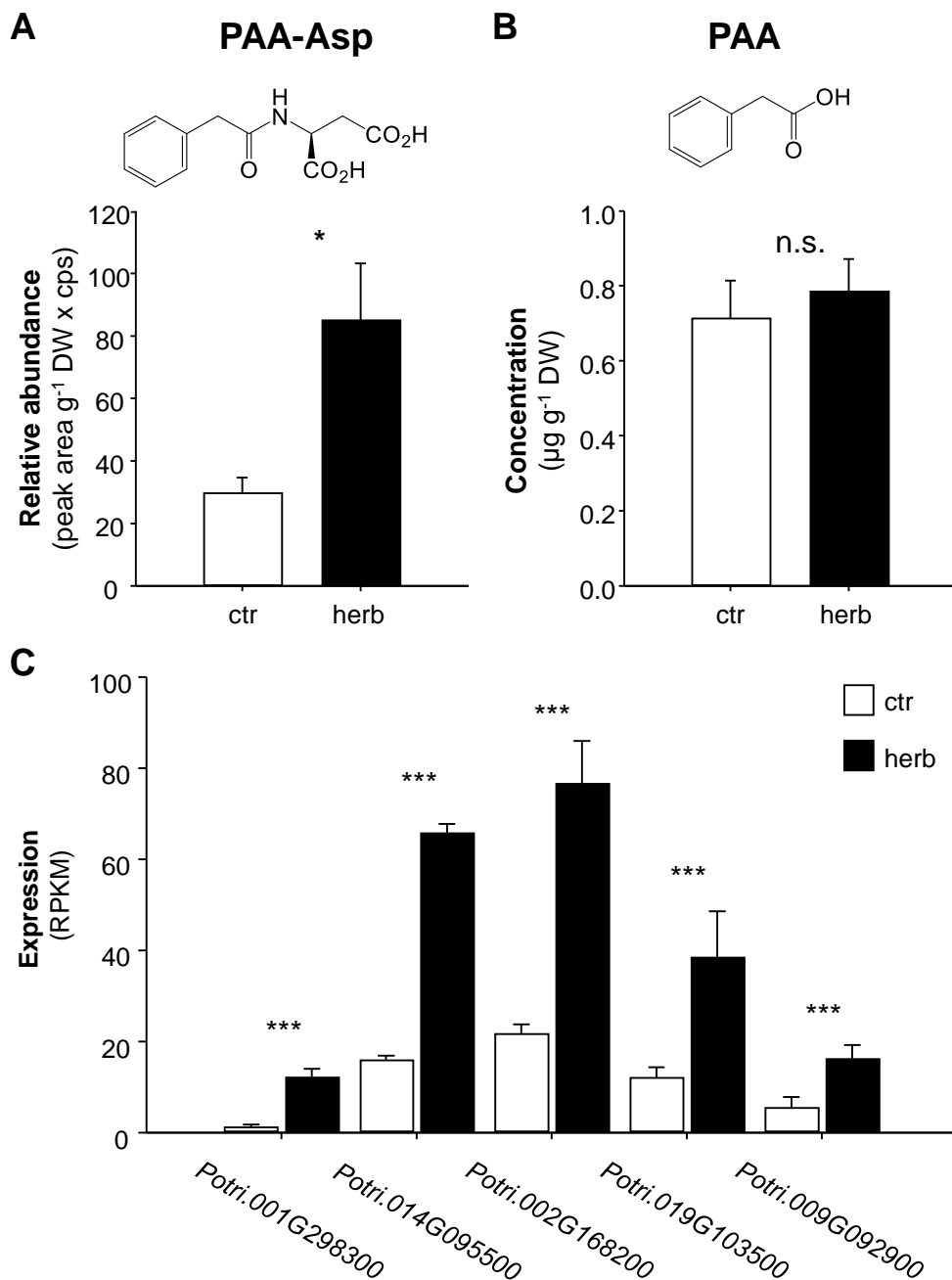


**Figure 3: Auxin, auxin conjugate and putative auxin-amido synthetase GH3 transcripts accumulate in herbivore-damaged leaves of *Populus trichocarpa*.**

Accumulations of PAA-Asp (A) and phenylacetic acid (B), were analyzed in *L. dispar* damaged (herb) and undamaged control (ctr) leaves of *Populus trichocarpa* via LC-MS/MS. Asterisks indicate statistical significance in Student's t-test or in Mann-Whitney Rank Sum Tests. PAA ( $P = 0.608$ ,  $t = -0.522$ ); PAA-Asp ( $P = 0.011$ ,  $t = -2.816$ ). Putative auxin-amido synthetase *GH3* Gene expression (C) in herbivore-damaged and undamaged leaves was analyzed by Illumina HiSeq sequencing. Expression was normalized to RPKM. Significant differences in EDGE tests are visualized by asterisks. Means  $\pm$  SE are shown ( $n = 4$ ). *Potri.001G298300* ( $P = 2.22705E-10$ , weighted difference (WD) =  $1.71922E-05$ ); *Potri.014G095500* ( $P = 4.04229E-20$ , WD =  $7.9334E-05$ ); *Potri.002G168200* ( $P = 1.01033E-12$ , WD =  $8.83786E-05$ ); *Potri.019G103500* ( $P = 1.39832E-05$ , WD =  $4.27809E-05$ ); *Potri.009G092900* ( $P = 5.97467E-05$ , WD =  $1.72578E-05$ ). Means  $\pm$  SE are shown ( $n = 10$ ). DW, dry weight. n.s. – not significant.

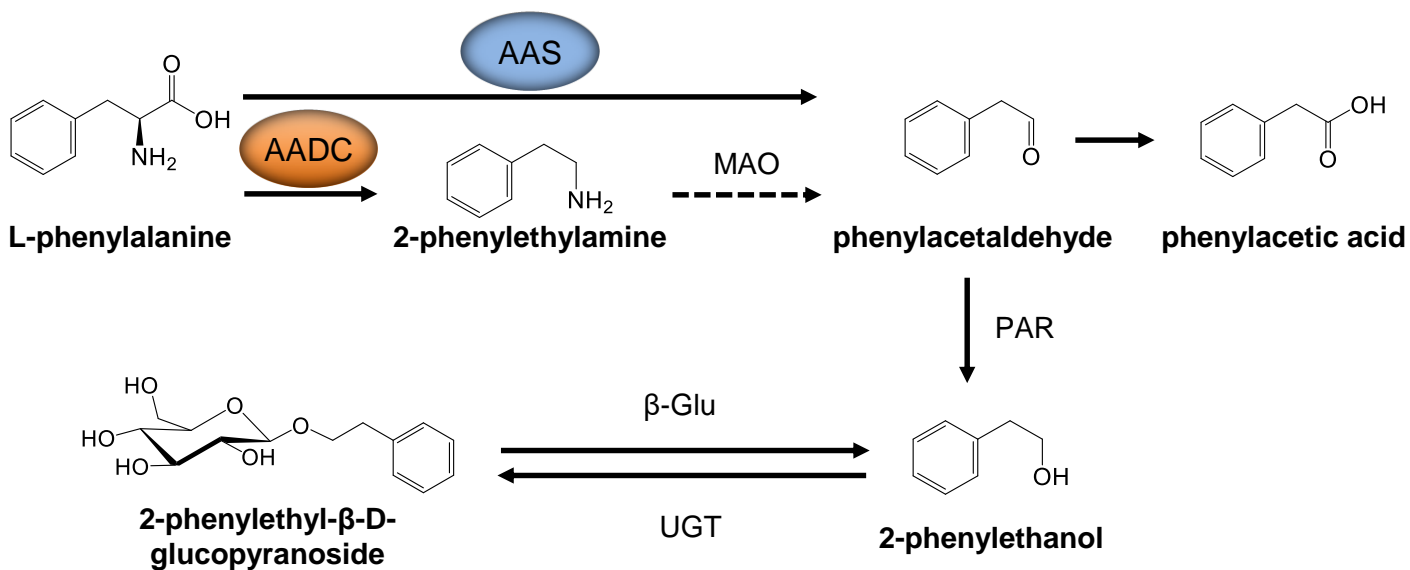
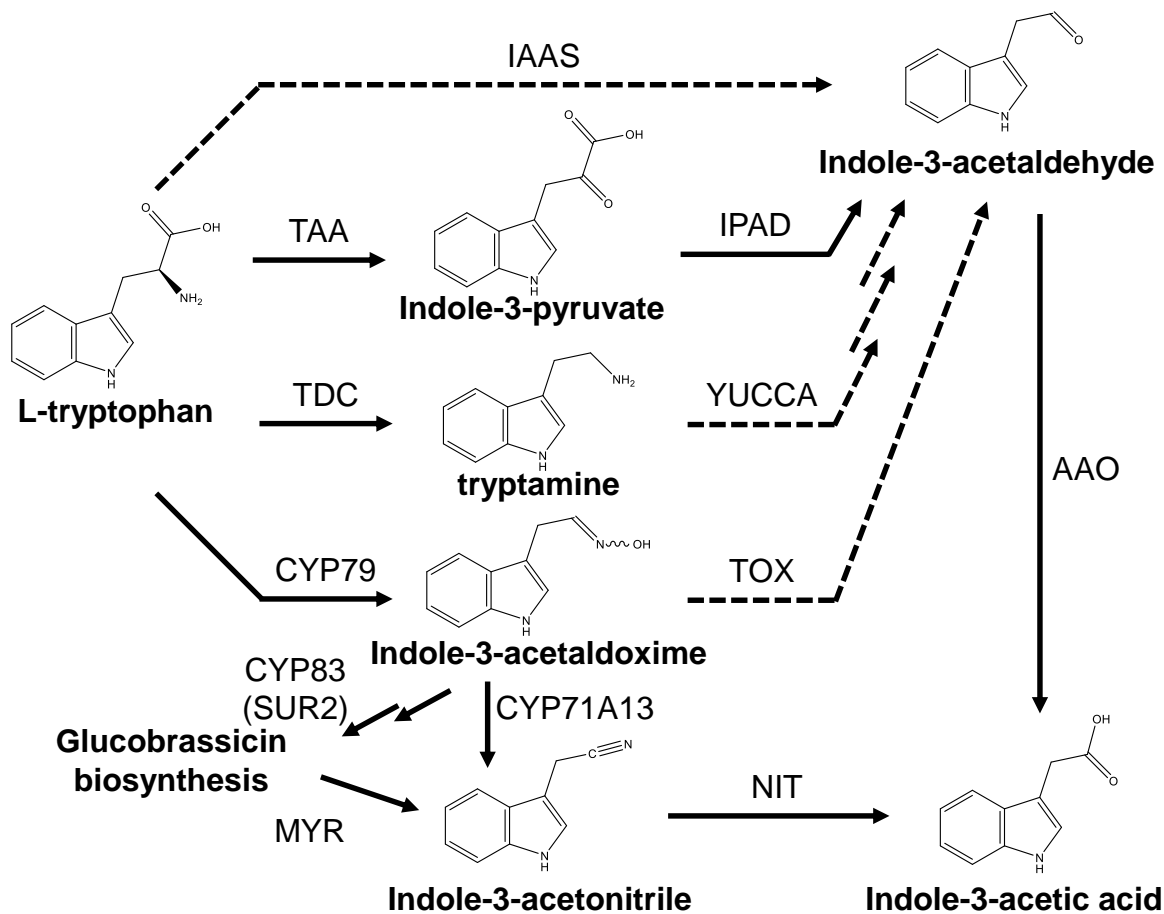


**Figure 4: Proposed pathways for the convergent biosynthesis of PAA in planta.**

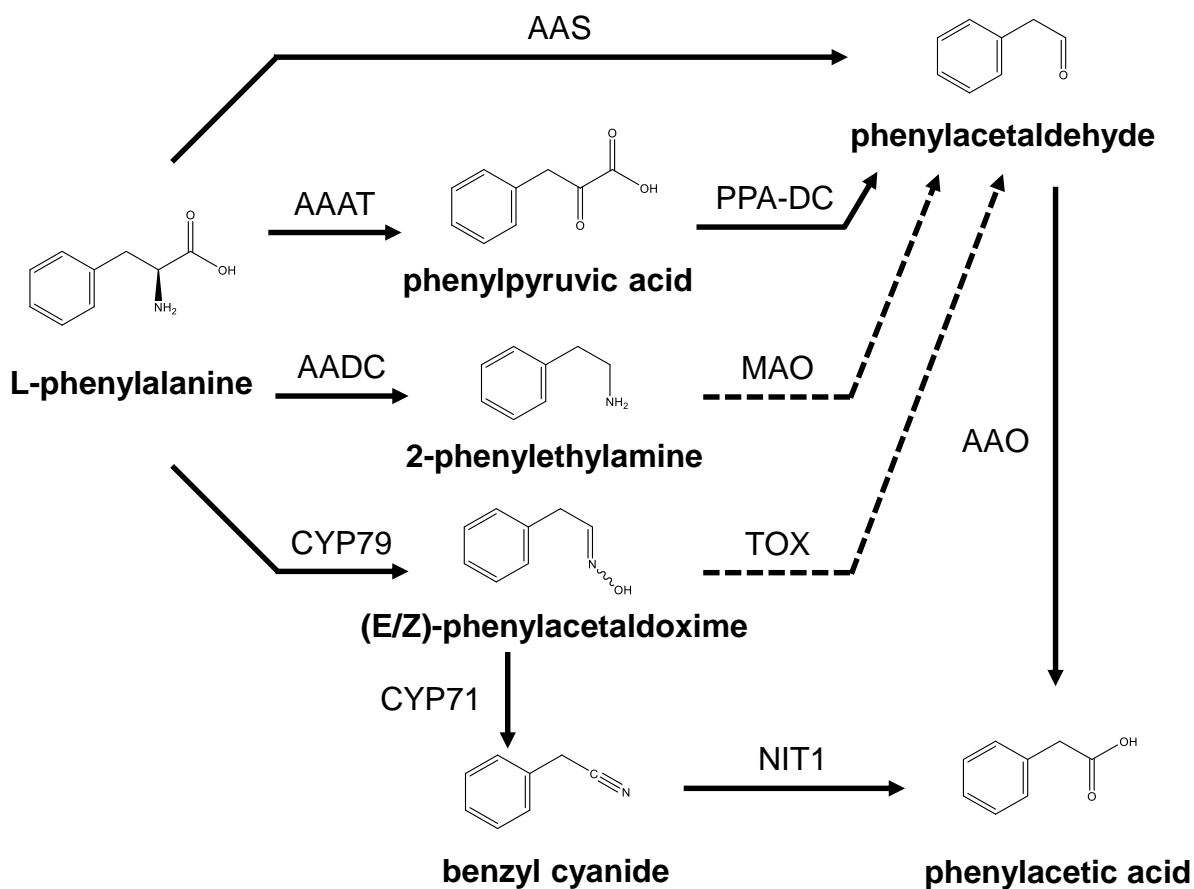
Convergent biosynthesis of 2-phenylethanol that can be initiated by AAS and AADC enzymes has been described. The initiation of the formation of phenylacetaldehyde as common substrate of 2-phenylethanol might also serve as substrate for the biosynthesis of the auxin PAA. Respective enzymes have been elucidated *in planta*. AADC, aromatic amino acid decarboxylase; AAS, aromatic aldehyde synthase; MAO, monoamine oxidase; PAR, phenylacetaldehyde reductase; UGT, UDP-glucosyl transferase; β-Glu, β-glucosidase. Dashed arrow, enzymes uncharacterized *in planta*. Solid lines, enzymes characterized *in planta*.



**Supplemental Figure 1: Proposed, simplified pathways for the biosynthesis of indole-3-acetic acid in plants.**

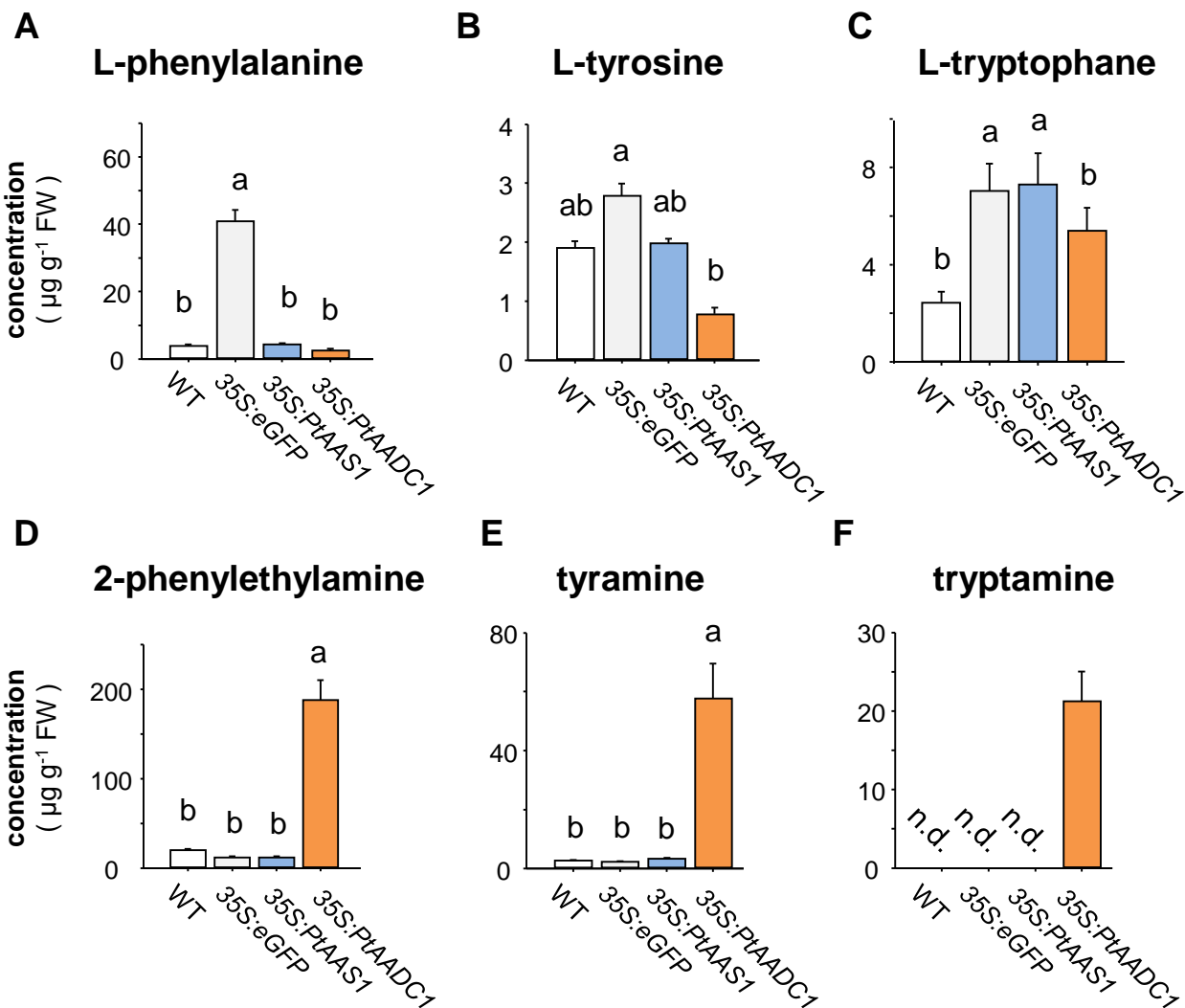
TAA, tryptophan aminotransferase; TDC, tryptophan decarboxylase; CYP79, cytochrome P450 family 79 enzyme; IAAS, indole-3-acetaldehyde synthase; IPA-DC, Indole-3-pyruvic acid decarboxylase; TOX, transoximase; AAO, aromatic aldehyde synthase; YUCCA, flavin monooxygenase-like enzyme; MYR, myrosinase; CYP83, cytochrome P450 family 83 enzyme; IPAD, indole-3-pyruvic acid decarboxylase. Dashed arrows, enzymes not characterized in plants; solid arrows, enzymes characterized in plants.





**Supplemental Figure 2: Proposed pathways for the biosynthesis of phenylacetic acid in plants.**

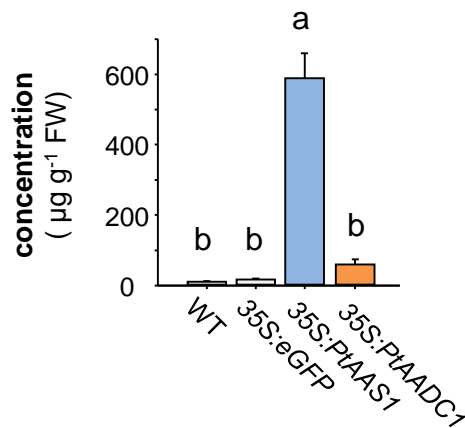
AAAT, aromatic amino acid transaminase; AADC, aromatic amino acid decarboxylase; CYP79, cytochrome P450 family 79 enzyme; PAAS, phenylacetaldehyde synthase; PPA-DC, phenylpyruvic acid decarboxylase; MAO, monoamine oxidase; TOX, transoximase; PAR, phenylacetaldehyde reductase; UGT, UDP-glucosyl transferase;  $\beta$ -Glu,  $\beta$ -glucosidase. Dashed line, enzymes not characterized in plants; solid line, enzymes characterized in plants.



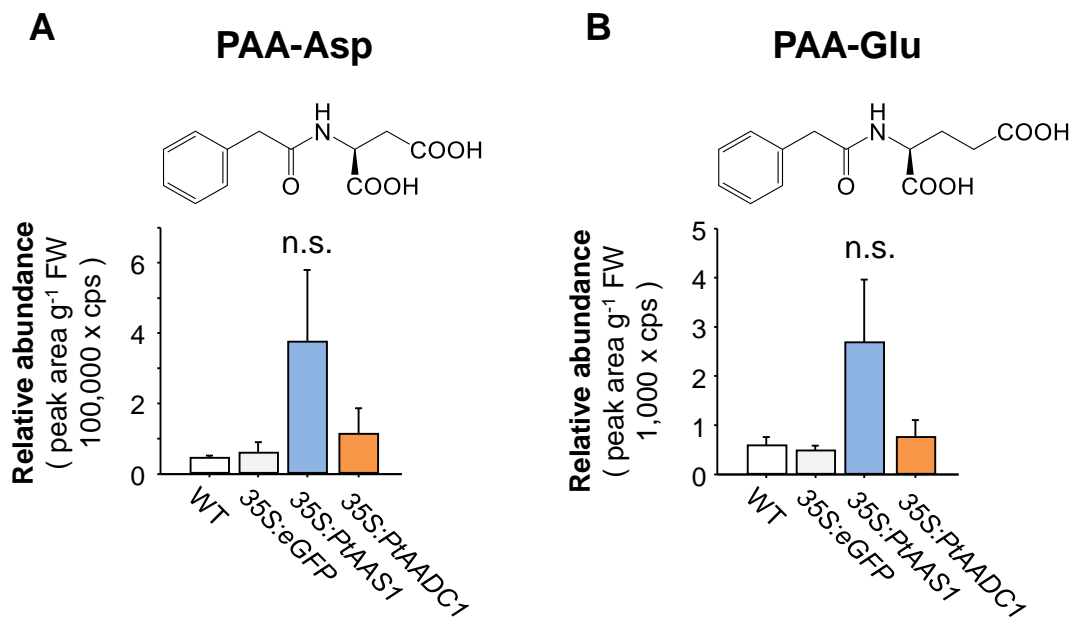
**Supplemental Figure 3: Expression of *PtAADC1* results in decreased aromatic amino acid substrate pools (A-C) and accumulation of aromatic amine products (D-F) in *N. benthamiana* leaves.**

The expression of poplar *PtAADC1* leads to the depletion of the aromatic amino acid substrates L-phenylalanine (A), L-tyrosine (B), and L-tryptophane (C) in expressing leaves. Accordingly, the corresponding enzymatic reaction products phenylethylamine (D), tyramine (E), and tryptamine (F) accumulate in *N. benthamiana* leaves, respectively. Different letters above each bar indicate statistically significant differences in Kruskal-Wallis One Way ANOVA and are based on the following Tukey test. Phe ( $H = 16.58$ ,  $P \leq 0.001$ ); Tyr ( $F = 32.883$ ,  $P \leq 0.001$ ); Trp ( $F = 73.043$ ,  $P \leq 0.001$ ); PEA ( $H = 19.167$ ,  $P \leq 0.001$ ); TyrA ( $H = 17.34$ ,  $P \leq 0.001$ ). Means  $\pm$  SE are shown ( $n = 6$ ). FW, fresh weight. n.d., not detected.

## 2-phenylethyl- $\beta$ -D-glucopyranoside

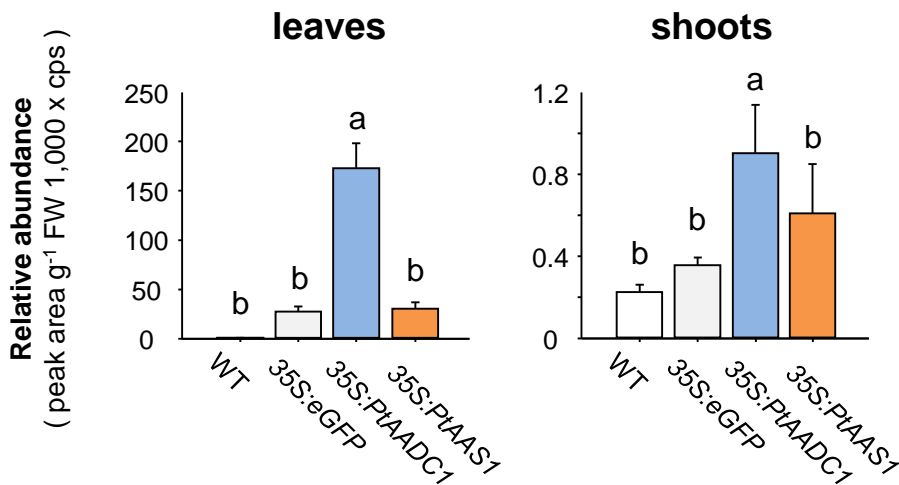
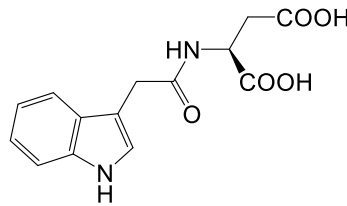


**Supplemental Figure 4: Expression of *PtAADC1* and *PtAAS1* results in the increased accumulation of 2-phenylethyl- $\beta$ -D-glucopyranoside in *N. benthamiana* leaves.** *N. benthamiana* plants expressing *eGFP*, *PtAAS1*, *PtAADC1* and wild type plants were grown for 5 days post inoculation as described (Günther et al., 2019). The accumulation of 2-PEG in *N. benthamiana* leaves was analyzed via LC-MS/MS. Different letters above each bar indicate statistically significant differences in Kruskal-Wallis One Way ANOVA and Tukey test. 2-PEG ( $H = 20.24$ ,  $P \leq 0.001$ ). Means  $\pm$  SE are shown ( $n = 6$ ). FW, fresh weight.

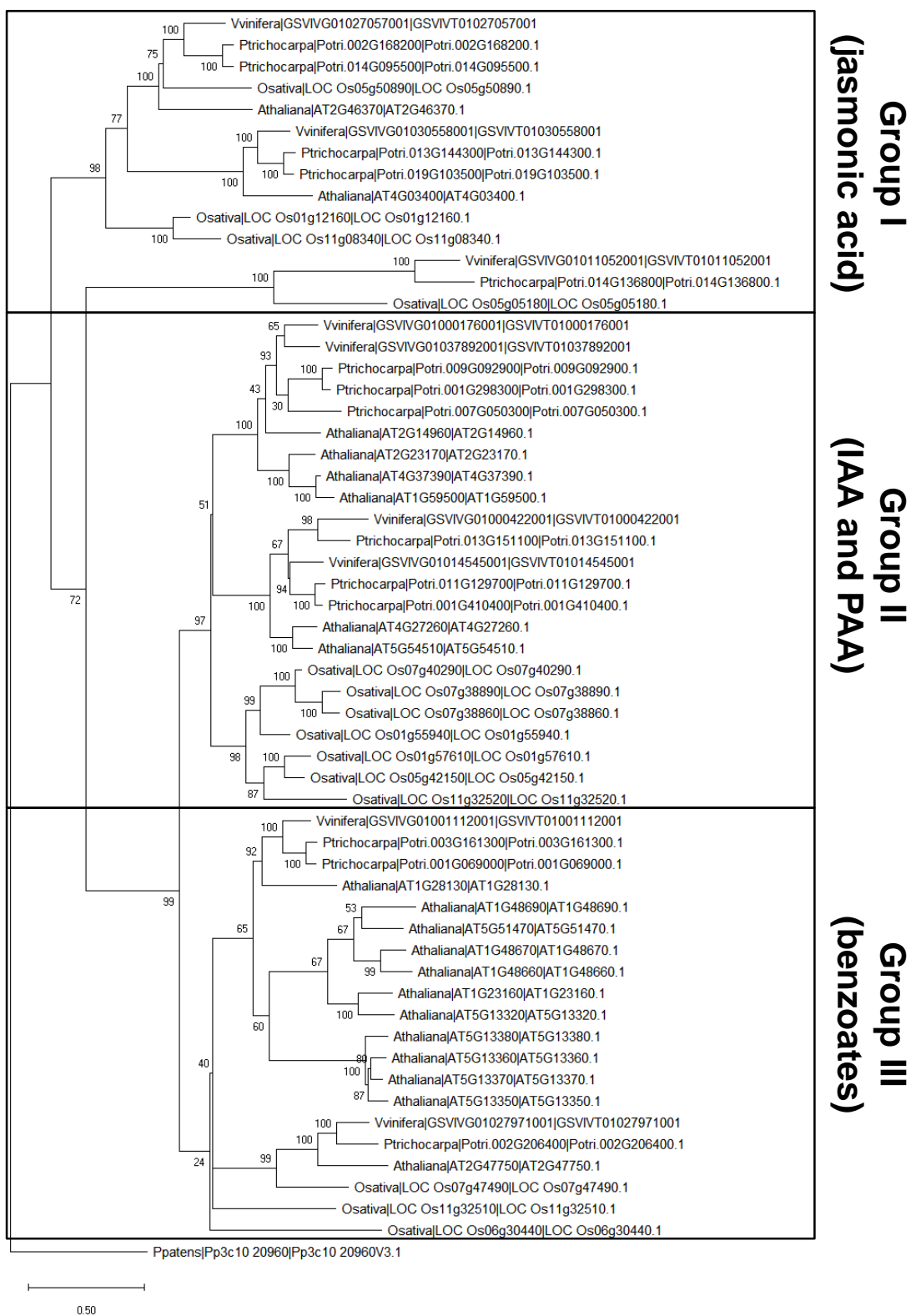


**Supplemental Figure 5: Expression of *PtAAS1* results in unaltered abundance of auxin conjugates PAA-Asp (A) and PAA-Glu (B) in *N. benthamiana* roots.** The identified conjugates were analyzed for a characteristic fragmentation via LC-MS/MS. Means + SE are shown (n = 6). FW, fresh weight. n.s., not significant

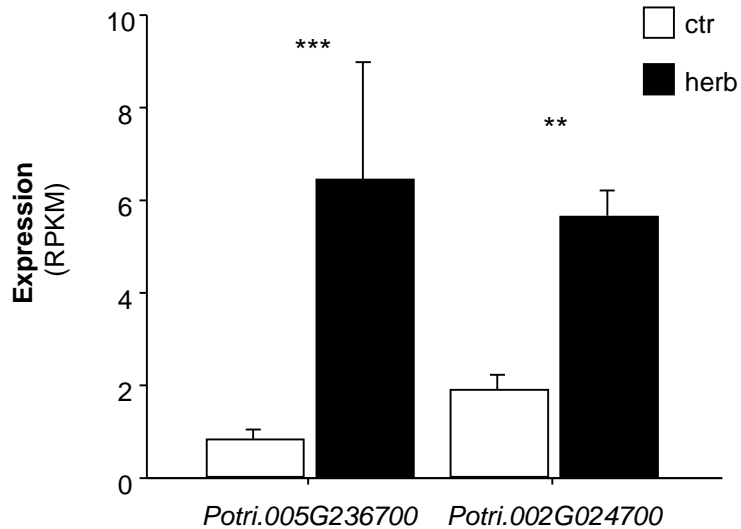
## IAA-Asp



**Supplemental Figure 6: Expression of *PtAAS1* results in increased levels of the auxin conjugate IAA-Asp in *N. benthamiana* shoots and leaves.** The identified conjugates were analyzed for a characteristic fragmentation via LC-MS/MS. Relative quantification of the identified conjugates IAA-Asp. Different letters above each box indicate statistically significant differences in Kruskal-Wallis One Way ANOVA and are based on the following Tukey test. IAA-Asp<sub>Shoots</sub> (H = 15.173, P = 0.002); IAA-Asp<sub>Leaves</sub> (H = 19.547, P ≤ 0.001). Means ± SE are shown (n = 6) FW, fresh weight.



**Supplemental Figure 7: Phylogenetic reconstruction of identified and characterized GH3 auxin-amido synthetases coding sequences.** Putative GH3 auxin-amido synthetase sequences from *Populus trichocarpa* and recently identified and characterized GH3 auxin-amido synthetases from *Oryza sativa*, *Arabidopsis thaliana*, and *Vitis vinifera*. Each group I - III is highlighted in rectangles and labeled with characteristic substrates. A putative GH3 from *Physcomitrella patens* served as outgroup. The tree was inferred by using the maximum likelihood method and  $n = 1,000$  replicates for bootstrapping. Bootstrap values are shown next to each node. Relative branch lengths measure the number of substitutions per site.



**Supplemental Figure 8: Transcript accumulation of *Aux/IAA* genes in *L. dispar*-damaged and undamaged *Populus trichocarpa* leaves.** Gene expression in herbivore-damaged (herb) and undamaged (ctr) leaves was analyzed by Illumina sequencing and mapping the reads to the transcripts of the *P. trichocarpa* genome version v3.0. Expression was normalized to RPKM. Significant differences in EDGE tests are visualized by asterisks. Means  $\pm$  SE are shown (n = 4). *Potri.005G236700* (P = 4.06063E-05, weighted difference (WD) = 8.81922E-06); *Potri.002G024700* (P = 0.005250486, WD = 6.0016E-06).